



Modeling the effects of yarn material properties and friction on the ballistic impact of a plain-weave fabric

M.P. Rao^{a,1}, Y. Duan^{a,2}, M. Keefe^{b,*}, B.M. Powers^c, T.A. Bogetti^c

^aCenter for Composite Materials, University of Delaware, Newark, DE 19716, USA

^bDepartment of Mechanical Engineering, University of Delaware, Newark, DE 19716, USA

^cUS Army Research Laboratory, Aberdeen Proving Ground, MD 21005, USA

ARTICLE INFO

Article history:

Available online 28 November 2008

Keywords:

Ballistic impact
Yarn material properties
Friction
Woven fabric
Finite element analysis

ABSTRACT

Impact of a rigid sphere onto a high-strength plain-weave Kevlar KM2® fabric was modeled using LS-DYNA® focusing on the influence of friction and material properties on ballistic performance. Quasi-static friction was experimentally determined and incorporated into the model. Two clamped edges and two free edges were used as boundary conditions to correlate the model to an experimental test providing yarn–yarn movement. Yarns were modeled as continua with modulus and strength dominating along the length. Parametric studies incorporating different yarn material properties and initial projectile velocities were then performed with the above set of boundary conditions. Results indicate that ballistic performance depends upon friction, elastic modulus and strength of the yarns. While friction improves ballistic performance by maintaining the integrity of the weave pattern, material properties of the yarns have a significant influence on the effect of friction. It is shown that fabrics comprised of yarns characterized by higher stiffness and strength relative to the baseline Kevlar KM2®, exhibited a stronger influence on ballistic performance. Therefore all three parameters viz., friction, elastic modulus and strength along with other variables (fabric architecture, boundary conditions, and projectile parameters) are needed to examine ballistic performance of high-strength fabric structures.

© 2008 Elsevier Ltd. All rights reserved.

1. Introduction

High-strength fabrics are often used in ballistic impact protection systems where flexibility and lightweight are of importance. Experiments demonstrate that interfacial friction affects the ballistic impact energy absorption of these fabrics [1–3]. Tan et al. [1] studied the ballistic performance of single layers of Twaron fabric. In their experiments, projectiles with different shapes were used to impact onto rectangular fabric specimens clamped along two opposite edges. Their experiments indicate that the energy expended in setting the yarns into motion and pushing them out of the way of the advancing projectile and overcoming projectile–fabric friction is a mechanism of energy absorption during impact. Briscoe and Motamedi [2] explored the frictional characteristics of three different styles of Kevlar fabric with respect to their ballistic impact performance. Different levels of inter fiber/yarn friction within the Kevlar fabrics were achieved by removal or addition of surface lubricants. It was found that for a given style of fabric, the

velocity required to perforate increased while the residual velocity decreased with increasing levels of friction. Fabric with a higher level of friction absorbs larger amounts of energy. Bazhenov [3] investigated the effect of water on the ballistic performance of a rectangular laminate comprised of 20 layers of Armos fabric. The specimens were attached to a plasticine foundation and struck with projectiles possessing spherical tips. The dry laminate stopped the bullet while the wet laminate was perforated. It was observed that the impacted yarns in the wet laminate were not broken indicating that the yarns moved laterally and allowed the bullet to slide through the fabric. Based on this observation, Bazhenov surmised that the water served as a lubricant that decreased friction between the bullet and the yarns.

Zeng et al. [4] developed a central difference based numerical model to study the effect of friction on woven fabric armor comprised of Twaron® CT716 fibers. In that work [4], the authors grouped inter-yarn friction as low ($\mu = 0.0\text{--}0.06$), moderate ($\mu = 0.06\text{--}0.2$) and high ($\mu = 0.2\text{--}1.0$) – based on the effect of friction on the energy absorption capacity of the fabric armor. They showed via detailed numerical simulations that the ballistic limit clearly increases in the low ($\mu = 0.0\text{--}0.06$) and moderate ($\mu = 0.06\text{--}0.2$) regimes, while in the high ($\mu = 0.2\text{--}1.0$) zone, the ballistic performance only very slightly diminishes. However, the authors of [4] surmise that increasing $\mu = 0.2$ to $\mu = 0.6$, yields little

* Corresponding author. Tel.: +1 302 831 8009; fax: +1 302 831 3619.

E-mail address: keefe@udel.edu (M. Keefe).

¹ Present address: Department of Mechanical and Aerospace Engineering, University of Florida, P.O. Box 116250, Gainesville, FL 32611-6250, USA.

² Present address: The Boeing Company, Seattle, WA, USA.

difference, but more importantly, determine that the optimum friction coefficient range for Twaron® CT716 woven fabrics is $0.1 \leq \mu \leq 0.6$.

Tan and Ching [5] developed a finite element model using bar elements to model the ballistic impact of a rigid sphere onto a plain-woven fabric structure made of Twaron® CT716 yarns. While the above study was successful in reducing the size of the problem, it did not account for the effect of changing material properties of the yarns coupled with friction. Barauskas and Abraitiene [6] developed a coupled shell and membrane element based finite element model of multi-layer fabric packages (MLFP) of plain-woven para-aramid Twaron® CT709 yarns under ballistic impact from a lead bullet. They showed that for the particular case modeled, acceptable results for wave propagation and residual projectile velocities were obtained in comparison with full detailed finite element simulations. While they did not explore the interplay between material properties and friction, they were successful in simulating the ballistic event between the lead projectile and a structure comprised of multiple layers of woven fabric. Naik and Shrira [7] developed a simplified analytical model to investigate the ballistic impact of plain-woven E-glass/epoxy and twill-woven T300 carbon/epoxy composite structures. The plain-woven E-glass/epoxy composite characterized by higher volumetric density, mode II dynamic critical strain energy release rate and fiber failure energy was shown to have a higher ballistic limit. However, they did not distinguish whether material properties or weave architecture had a greater contribution toward the observed ballistic performance. Tabiei and Ivanov [8] developed a computationally efficient micro-mechanics based material model for braided composites to interface with LS-DYNA. While their model accounts for yarn reorientation and interlocking, the spatially varying crimp of the yarns is approximated to be constant. The membrane shell elements based finite element model developed in [8], significantly reduces the size of the problem, and produces results in excellent agreement with experimental data. Yet, their study does not address the interaction between friction and material properties with respect to ballistic performance.

The experimental work presented in [1–3] clearly shows that interfacial friction plays a critical role in the ballistic impact of fabrics. However, the mechanisms through which friction takes effect are not well understood. In previous papers by Duan et al. [9,10], a finite element analysis (FEA) model was created to simulate the ballistic impact of a rigid sphere onto a square panel of plain-woven fabric. Projectile–fabric and yarn–yarn friction were taken into account as well as yarn failure. The effect of friction on the fabric energy absorption and the mechanisms through which friction plays a role were deduced from that modeling effort. However, friction was only parametrically modeled as either very large or not present and material properties were meant to show trends, but not represent actual materials. Further work by the authors [11] utilized material properties from actual Kevlar woven fabric and compared to experiments. However, in the above cited works [9–11], the effect of yarn material properties on the ballistic performance of woven fabrics has not been addressed. As such, it is postulated that friction along with yarn material properties could influence the ballistic performance.

Therefore, the present work endeavors to address the effects of both yarn material properties and friction. The effects of parametric variation of yarn mechanical properties viz.; elastic modulus and stress-to-failure are studied along with the effect of friction – both yarn–yarn and projectile–fabric. A novel pull-out test method is developed to compare static to dynamic friction and these experimental results are used in this work. These studies further demonstrate the inter-relationship of variables when studying ballistic impact and the importance of modeling when trying to understand this complex phenomenon.

2. Modeling the ballistic impact onto a plain-weave fabric

A commercially available explicit nonlinear FEA code, LS-DYNA, is used to model the ballistic impact of a rigid sphere onto a single layer of a high-strength fabric. Fig. 1 shows the initial geometry of the impact event: a 0.627 g, 5.35 mm diameter rigid steel sphere impacting at normal incidence onto the center of a 50.8 mm × 50.8 mm square plain-woven fabric panel of areal density 180 g/m² with 34 yarns per inch in the warp and fill directions. The projectile is constrained to move in the direction normal to the X-Z plane. The edges of the fabric are perpendicular to the warp/weft yarns with two edges clamped, two edges free. The projectile and fabric parameters are chosen based on tests performed at the Army Research Laboratory (ARL), Aberdeen Proving Ground, Maryland,

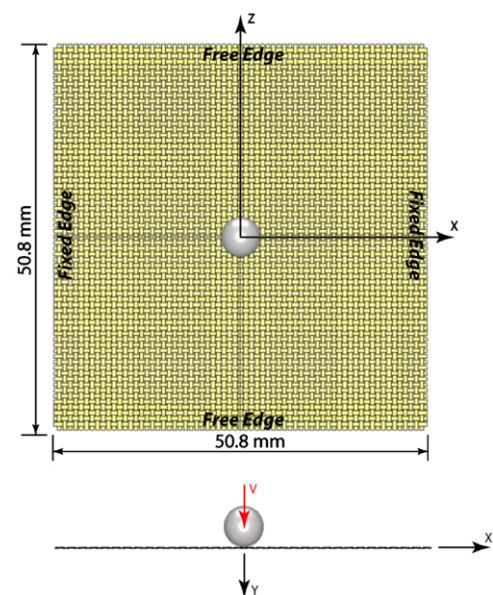


Fig. 1. Initial geometry of the simulated impact event.

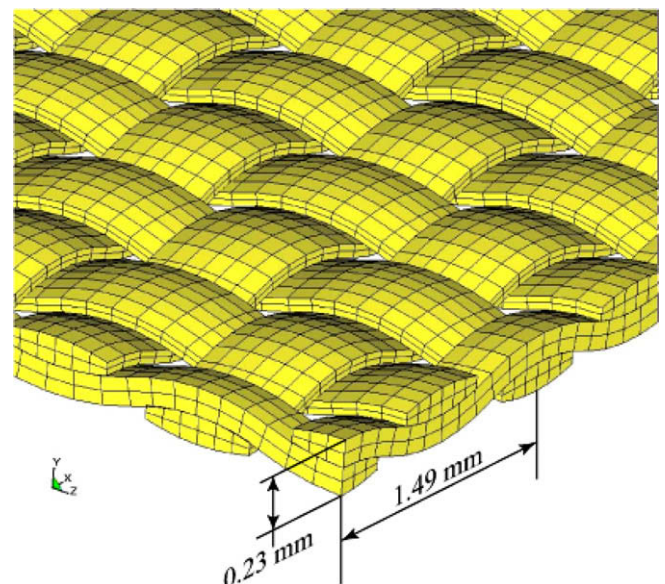


Fig. 2. Details of the quarter symmetric 3D finite element mesh of the initial geometry shown in Fig. 1.

using .22 caliber “Type F” shot against neat plain-woven 600 denier Kevlar KM2® fabric [11].

Since the impact system has symmetry with respect to the X-Y plane and the Y-Z plane, only a quarter of the entire system needs to be modeled. As in the previous papers by the authors [9–11], the fabric is modeled at a yarn level of resolution. The warp and fill yarns are modeled as transversely isotropic elastic continua and combined to form the fabric weave structure. Fig. 2 shows the details of the finite element mesh for the plain-woven fabric. Mesh sensitivity studies indicated that the chosen mesh density was able to capture both the longitudinal and transverse wave responses of the impact event. The fabric thickness is 0.23 mm and the yarn crimp wavelength is 1.49 mm. The material constants for the transversely isotropic Kevlar KM2® yarns are dominated by the longitudinal tensile modulus ($E_{11} = 62$ GPa) [12] assuming the 1-direction to be along the fiber axis. In these studies, the transverse elastic moduli (E_{22} and E_{33}) and shear moduli (G_{12} , G_{13} , and G_{23}) are assumed to be two and three orders of magnitude smaller than E_{11} , while the Poisson’s ratio are set as $\nu_{12} = \nu_{13} = \nu_{23} = 0$, since the yarns are collections of loose individual fibers. The density of

the yarn is modified from the density of Kevlar KM2® fibers using a simple tightest packing approach and assuming the Kevlar KM2® fibers in the yarns have a circular cross-section: a simple geometry of packing circles creates a tightest volume ratio of 0.91, leading to $\rho_{yarn} = 1310$ Kg/m³, as opposed to $\rho_{fiber} = 1440$ Kg/m³. Since the elastic modulus along the fiber direction (E_{11}) is much larger than the transverse and shear moduli, the von Mises stress at a material point is approximately equal to the stress in the fiber direction. The stress in the fiber direction is a linear function of the strain in that direction. Therefore, the maximum von Mises stress failure criterion is roughly equivalent to a maximum strain failure criterion, which has been used by other researchers for the investigation of yarns [14–16]. Consistent with the studies of Cheng et al. [13], the failure of Kevlar KM2® yarns is triggered if the maximum principal stress along the longitudinal direction $\sigma_1 \geq 3.4$ GPa.

2.1. Experimental friction measurement

Quasi-static yarn friction tests and yarn pull-out tests are used to characterize the friction behavior between Kevlar KM2® yarns. A



Fig. 3. Test fixture and setup for the yarn pull-out experiments.

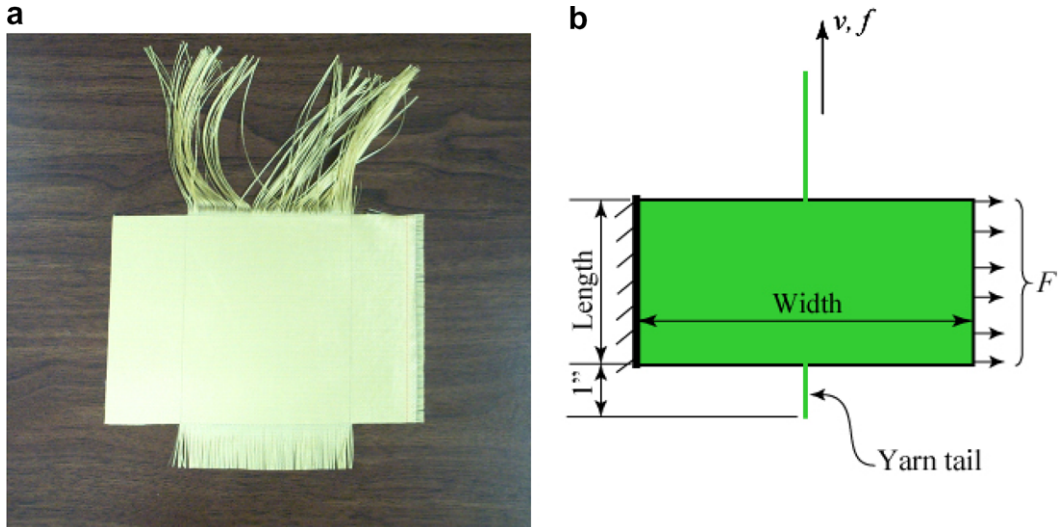


Fig. 4. (a) Photograph of the Kevlar KM2® fabric employed during ballistic experiments. (b) Schematic representation of the yarn pull-out test.

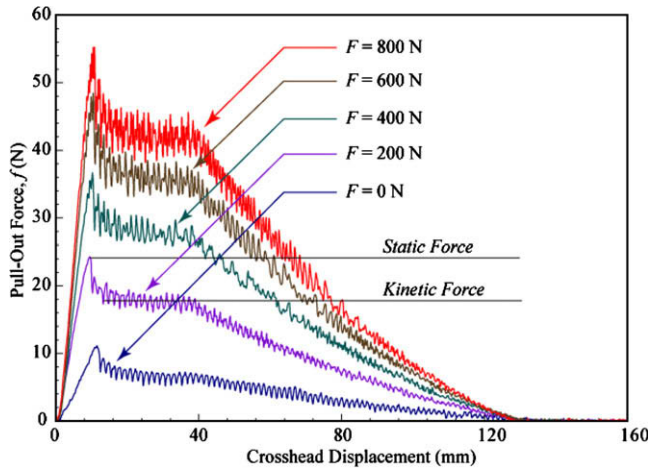


Fig. 5. Yarn pull-out force measured as function of crosshead displacement for varying magnitudes of the applied pre-load, F .

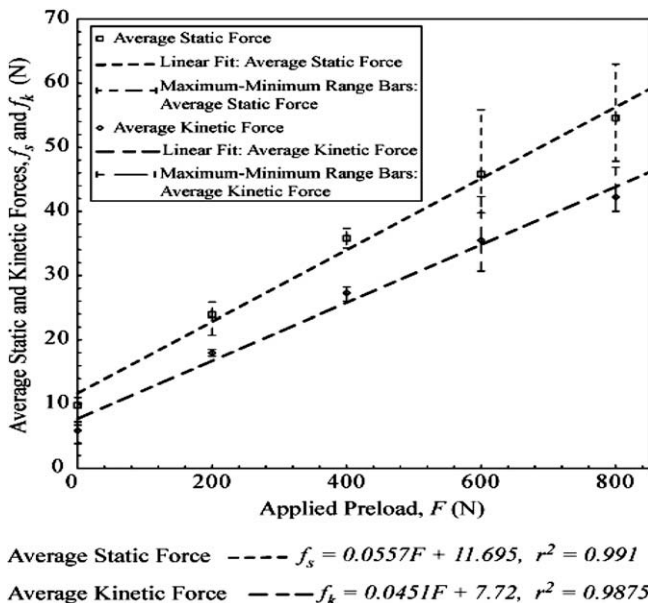


Fig. 6. Average static and kinetic forces obtained from the yarn pull-out tests performed with the baseline Kevlar KM2® fabric.

simple system for pulling one yarn against another with known loads allows a direct measurement of yarn–yarn friction coefficients, and yarn pull-out tests, uniquely performed using a non-woven ‘tail’ on the pulled yarn, allow incorporation of the geometry effects of the weave into the friction modeling. Fig. 3 shows a test fixture developed previously at ARL for yarn pull-out tests. This fixture uses springs to provide a pre-load along the width of the fabric while using a standard force-displacement device to perform the load vs. displacement measurements of a yarn pull-out from the fabric. Fig. 4a shows a 600 denier Kevlar KM2® test sample with the modified yarn ‘tail.’ Different specimens, characterized by the dimensions indicated in Fig. 4b, were used to perform individual pull-out tests. Using an approach similar to Coulomb friction, one could write:

$$f = \mu F \quad (1)$$

where f is the pull-out force, F is the applied pre-load perpendicular to the pull-out force, and μ is a coefficient of friction between the individual Kevlar KM2® yarns.

Fig. 5 shows typical results for various pre-loads in the width direction corresponding to a Kevlar KM2® specimen. Five specimens were employed to obtain five sets of data similar to the results in Fig. 5. The static and kinetic forces for each data set were averaged as shown in Fig. 5, and these averages (along with maximum and minimum bounds) are reported in Fig. 6 as functions of applied pre-load. It is clear from Fig. 6 that individual linear relationships could be employed to predict both the average kinetic and static forces of friction in terms of the applied pre-load.

The above linear trend line equations can be written as:

$$f_s = m_s F + d_s \quad (2)$$

$$f_k = m_k F + d_k \quad (3)$$

In Eqs. (2) and (3), f_s and f_k are the average static and kinetic yarn pull-out forces, m_s and m_k , are the slopes of the two trend lines, F indicates the applied pre-load, and d_s and d_k , represent the intercepts of the two trend lines. Differentiating the above equations with respect to F , enables one to relate the slopes of the trend lines as:

$$\frac{m_s}{m_k} = \frac{df_s}{df_k} \quad (4)$$

Now, making use of Eq. (1) for both static and kinetic cases, one can derive:

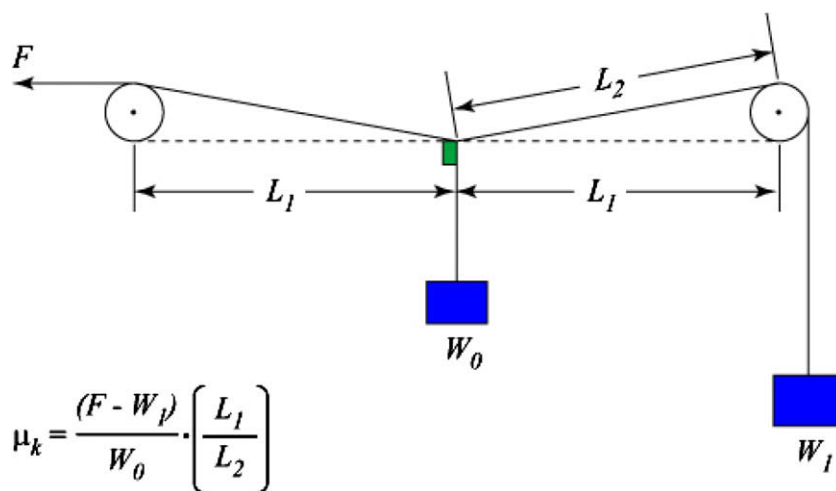


Fig. 7. Schematic representation of the friction device designed to measure the yarn–yarn and yarn–wire coefficient of kinetic friction.

$$\frac{df_s}{df_k} = \frac{\mu_s dF}{\mu_k dF} \quad (5)$$

where, in Eq. (5), μ_s and μ_k are the coefficients of static and kinetic friction between the individual Kevlar KM2® yarns. Equating Eqs. (4) and (5) gives:

$$\mu_k = \frac{m_k}{m_s} \mu_s \quad (6)$$

Fig. 7 shows a schematic of a simple test system where a yarn is pulled horizontally while a weighted yarn loop uses gravity to provide a transverse load. Experiments performed on the test system shown in Fig. 7 using Kevlar KM2® yarns and a steel wire to suspend the weight W_0 , indicated a kinetic coefficient of friction in the range $0.15 \leq \mu_k \leq 0.20$. However, the test results shown in Fig. 8 indicate that the kinetic friction coefficient, μ_k , between a Kevlar KM2® yarn and a steel wire converges to a value of approximately 0.18, as the weight W_0 is increased. Data obtained by using Kevlar KM2® yarns for the pulled yarn and the yarn loop in Fig. 7, showed trends similar to those reported in Fig. 8 for Kevlar KM2® yarns and a steel wire.

Using the experimental approach discussed above, a kinetic coefficient of $\mu_k = 0.19$ was determined between Kevlar KM2® yarns. Eq. (6) and the results from Fig. 6 can now be used with that experimentally determined μ_k to estimate μ_s , the static coefficient of friction, as $\mu_s = 0.23$ for Kevlar KM2® yarns. Based on the work of Zeng et al. [4], Twaron® fibers are similar to Kevlar®, and as such, the chosen magnitudes of μ_k and μ_s are within $0.1 \leq \mu \leq 0.6$ – the range of optimum coefficient of friction. It should be noted however, that Zeng et al. [4] do not make a distinction between kinetic and static coefficients of friction. Additionally, Briscoe and Motamedi [2] experimentally determined the coefficient of friction for Kevlar 49 yarns as $\mu = 0.22 \pm 0.03$ using a hanging-yarn configuration for yarn–yarn friction measurements. In light of the work reported in [2–4], the magnitudes of $\mu_k = 0.19$ and $\mu_s = 0.23$, employed in the simulations reported in this study appear to be reasonable.

Yarn pull-out test results presented in Fig. 5 indicate that the transition from static friction to stable kinetic friction is very sharp – implying that the friction between Kevlar KM2® yarns exhibits stable kinetic friction behavior once there is a small relative

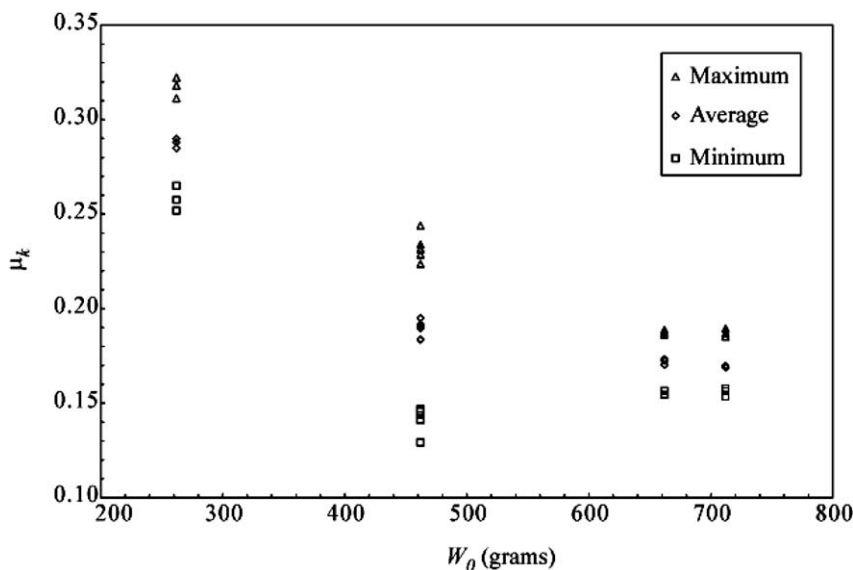


Fig. 8. Coefficient of kinetic friction between the Kevlar KM2® yarn and the steel wire.

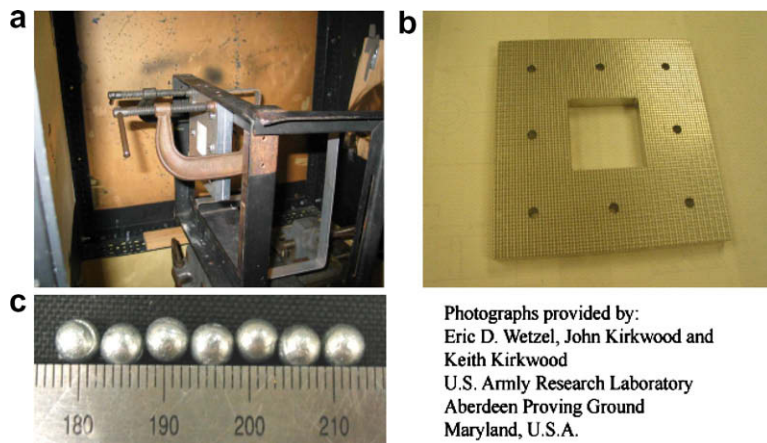


Fig. 9. The fabric ballistic impact test fixture designed and developed at ARL. (a) Fabric clamping fixture in gas gun range. (b) Aluminum fabric clamping fixture with knurled faces. (c) Steel balls used for ballistic testing.

Photographs provided by:
Eric D. Wetzel, John Kirkwood and
Keith Kirkwood
U.S. Army Research Laboratory
Aberdeen Proving Ground
Maryland, U.S.A.

Table 1

V_s/V_r data for the baseline Kevlar KM2® fabric. “N/P” implies “No Penetration”, while “N/A” indicates fabric perforation but unavailability of V_r .

Shot number	V_s (m/s)	V_r (m/s)	Projectile mass (g)
3	60.6	N/P	0.6230
12	92.1	N/A	0.6210
25	120.7	N/A	0.6260
28	121.2	N/A	0.6044
29	181.2	N/A	0.6356
30	245.0	207.1	0.6275

Table 2

The material and frictional parameters modeled in this study.

Material	Stiffness (GPa)	Strength (GPa)
<i>Material parameters</i>		
Kevlar KM2®	$E_{11}^{\text{Kevlar}} = 62.0$	$\sigma_1^{\text{KevlarKM2}} = 3.4$
Material2	$E_{11} = 2^*E_{11}^{\text{Kevlar}}$	$\sigma_1 = 1.5\sigma_1^{\text{KevlarKM2}}$
Material3	$E_{11} = E_{11}^{\text{Kevlar}}$	$\sigma_1 = 1.5\sigma_1^{\text{KevlarKM2}}$
Material4	$E_{11} = 2^*E_{11}^{\text{Kevlar}}$	$\sigma_1 = \sigma_1^{\text{KevlarKM2}}$
<i>Friction interactions</i>		
Projectile-fabric and yarn-yarn	Yarn-Yarn	Projectile-Fabric

For each material, the four frictional interactions mentioned above could potentially be treated individually resulting in a total of 16 simulations at a given striking velocity.

velocity between the two surfaces in contact. The effective friction coefficient μ between two contact surfaces is modeled using an exponential formulation as in Eq. (7) below [17]:

$$\mu = \mu_k + (\mu_s - \mu_k) \cdot e^{-\alpha|v_{rel}|} \quad (7)$$

In Eq. (7), μ_k is the stable kinetic friction coefficient, μ_s is the static friction coefficient, $|v_{rel}|$ is the relative velocity between two surfaces in contact, and α is an exponential decay coefficient describing the transition from static friction to stable kinetic friction. Since the transition from static friction to stable kinetic friction is very sharp for the Kevlar KM2® yarns, the exponential decay coefficient α is set equal to 10^8 – a large positive number.

The relative velocity between the projectile and the fabric is very high owing to the high incident velocity. Essentially, the second term in Eq. (7) is near zero in this case, and as such it is assumed that the frictional behavior between these contacting entities is effectively represented by a simple constant coefficient of friction. Therefore for projectile-fabric friction we set $\mu_k = \mu_s = 0.18$ based on the results reported in Fig. 8.

2.2. Model parameters

The projectile striking velocity (V_s) for simulating ballistic impact onto the baseline 600 denier Kevlar KM2® woven fabric was obtained experimentally. The test fixture [11] used for this purpose is presented in Fig. 9, and the measured striking and residual (V_r) velocities are reported in Table 1. The data reported in Table 1 enables one to surmise that $60.6 \text{ m/s} \leq V_{50} \leq 92.1 \text{ m/s}$, since at $V_s = 60.6 \text{ m/s}$, the projectile does not penetrate this Kevlar KM2® fabric, whereas at $V_s = 92.1 \text{ m/s}$, the fabric is penetrated. The above relation does not indicate that $V_{50} = V_s$ for the particular fabric. Rather, it implies a range for the V_{50} velocity, since by definition, at the V_{50} there is a 50% probability that the fabric will be perforated.

For model calibration, simulations were then performed by varying the velocity of the projectile until obtaining essentially zero residual velocity – that is, determining the initial velocity at which the projectile was just able to penetrate the fabric. If the predicted striking velocity against the baseline Kevlar KM2® fabric was within the range $60.6 \leq V_s \leq 92.1 \text{ m/s}$ for $V_r \cong 0$, then the model was considered to have been calibrated. For this purpose the yarn material and failure properties employed are those discussed in Section 2 above, while the coefficients of friction between various contacting entities were determined as discussed previously.

In order to assess the interaction between material properties and friction, the four different parametric cases presented in Table 2 were modeled in this study. As reported in Table 2, for each material property combination, four different frictional interactions are possible leading to a total of sixteen simulations at a given striking velocity. In order to maintain brevity of discussions however, Figs. 10 – 15 report on simulations at different striking velocities and combinations of material properties and frictional interactions as listed in Table 2.

3. Results

In ballistic impact experiments it is customary to measure the projectile striking velocity and residual velocity [2,14,18–20]. Beginning with $V_s = 55 \text{ m/s}$, simulations were run to $+5 \text{ m/s}$ changes in the striking velocity of the projectile, in most cases, and then simple interpolation was used to characterize the projectile velocity resulting in zero residual velocity. Fig. 10 shows the baseline Kevlar KM2® simulation for the cases with projectile-fabric and yarn-yarn friction as well as the cases with no friction at all. The projectile velocity time histories reported in Fig. 10 indicate that at $V_s = 60 \text{ m/s}$ with no friction at all between contacting

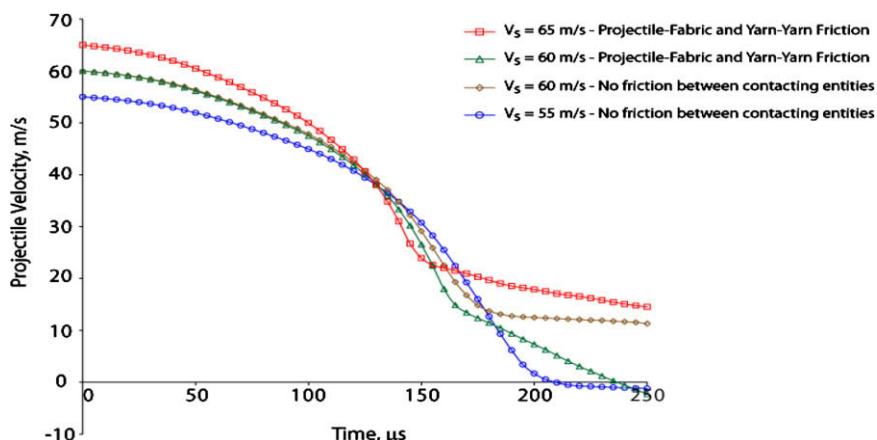


Fig. 10. The projectile velocity time history during the simulated impact event on the baseline Kevlar KM2® plain-woven fabric.

entities and at $V_s = 65$ m/s with projectile–fabric and yarn–yarn friction, V_r has a (small) positive magnitude – thus the fabric has been penetrated. On the other hand at $V_s = 55$ m/s with no friction at all between contacting entities and at $V_s = 60$ m/s with projectile–fabric and yarn–yarn friction, V_r has a negative magnitude – thus the projectile was stopped and it bounced back. Therefore friction aids in increasing the ballistic limit from 55 m/s to 60 m/s. Fig. 11 shows the result at the end of the simulation for the four different friction cases again with the Kevlar KM2® baseline material properties. Whereas projectile–fabric and yarn–yarn friction aid in localizing the damage region and maintaining integrity of the fabric (see Fig. 11a and b), the absence of friction (see Fig. 11c) and only projectile–fabric friction (see Fig. 11d) result in widespread damage and loss of fabric integrity. Figs. 12 and 13 re-

port results analogous to Figs. 10 and 11, respectively, however in this case, the fabric is comprised of Material2 (see Table 2) yarns. As seen from Fig. 12, the Material2 fabric is able to stop a projectile even at $V_s = 90$ m/s.

Table 3 summarizes the results for fabrics comprised of the baseline Kevlar KM2® and Material2 yarns. For the baseline Kevlar KM2® fabric $V_r \cong 0$ at $V_s = 56$ m/s with no friction between contacting entities and at $V_s = 61$ m/s with projectile–fabric and yarn–yarn friction. Therefore friction results in approximately 9% increase in the Kevlar KM2® baseline simulations with regards to the initial velocity of the projectile that will result in near zero residual velocity after impact – clearly there is a greater benefit to having friction between the yarns relative to friction between only the projectile and fabric. Comparing the ‘no friction’ and projectile–fabric and

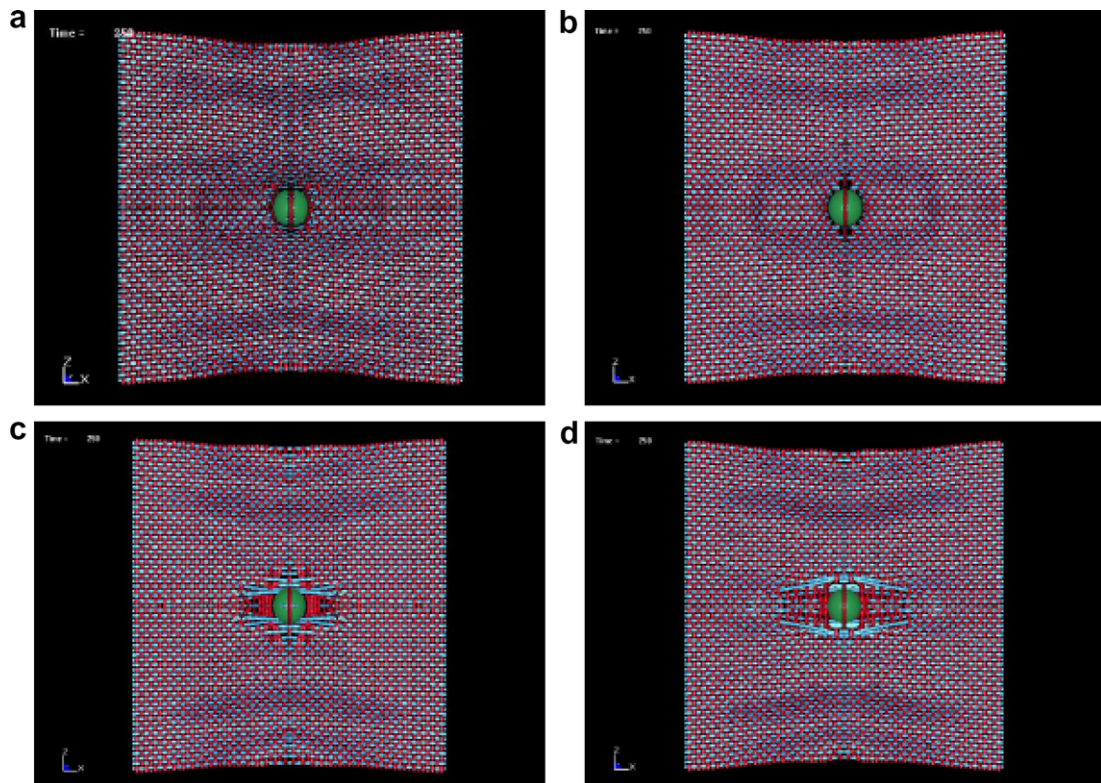


Fig. 11. Predicted damaged configuration of the back face of the baseline Kevlar KM2 fabric at 250 μ s, corresponding to the termination of the simulation. (a) Projectile–fabric and yarn–yarn friction at $V_s = 60$ m/s. (b) Only yarn–yarn friction at $V_s = 60$ m/s. (c) Friction not introduced between contacting entities at $V_s = 55$ m/s. (d) Only projectile–fabric friction at $V_s = 55$ m/s.

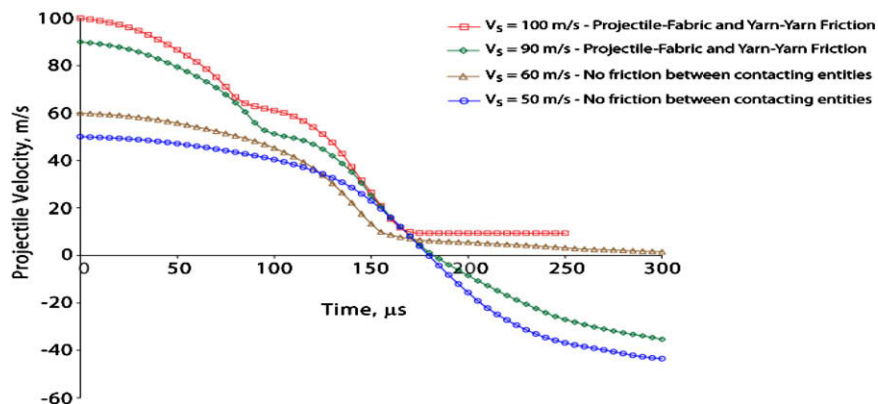


Fig. 12. The computed residual velocity of the projectile impacting on a fabric comprised of yarns characterized by Material2.

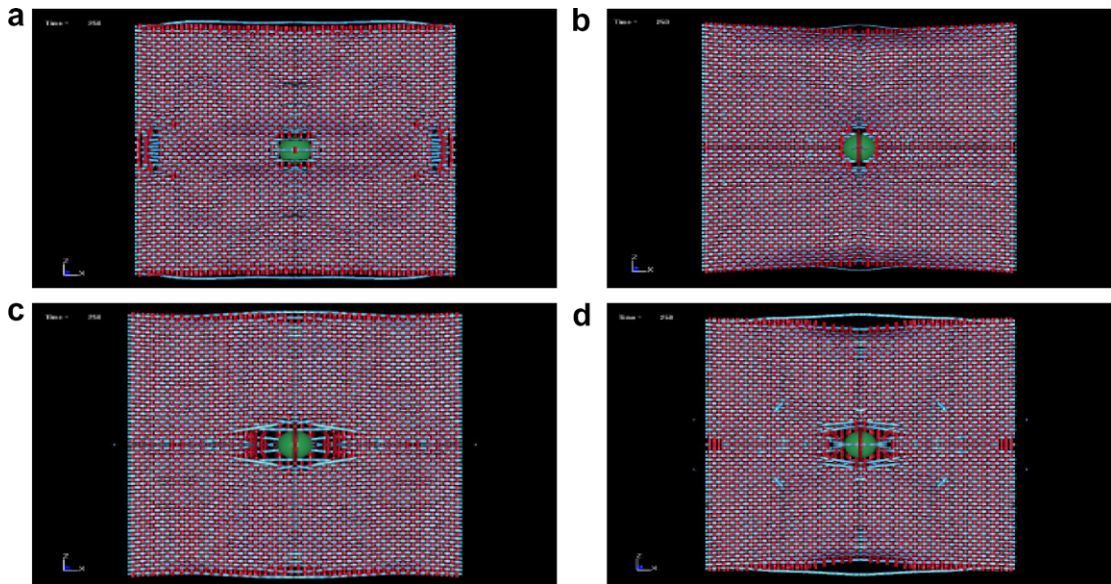


Fig. 13. The predicted back face degradation at 250 μ s of the fabric comprised of yarns characterized by Material2. (a) Projectile–fabric and yarn–yarn friction at $V_s = 100$ m/s. (b) Only yarn–yarn friction at $V_s = 70$ m/s. (c) Friction not introduced between contacting entities at $V_s = 60$ m/s. (d) Only projectile–fabric friction at $V_s = 70$ m/s.

yarn–yarn friction cases for Material2 (see Table 3b), it is evident that friction results in a 63% increase in the ability of this fabric to stop the projectile.

3.1. Failure mechanisms

It is interesting to note from Fig. 11, that the mode of failure in the absence and presence of friction is quite different – evident from the back face configuration of the fabric. Without friction between the yarns, there is noticeable movement of the yarns up to a few projectile diameters from the impact point, whereas with friction between the yarns, the projectile essentially causes only minor yarn–yarn movement.

However, there is clearly a difference between the fabrics comprised of Kevlar KM2® baseline and Material2 yarns. Although Figs. 11 and 13 show similar back face effects – that is, with friction between yarns there is noticeably less yarn–yarn movement away from the projectile, however as reported above, there is a significant improvement of over 63% in the ability of this fabric to stop the projectile. This improvement occurs only because of friction: without friction, with regards to the striking velocity (V_s) that will result in $V_r \approx 0$

after impact, this material has similar performance to the Kevlar KM2® baseline fabric, as seen from Table 3.

It is however, very important to note that the imposed boundary conditions (see Fig. 1) also cause different fabric failure conditions between the Kevlar KM2® baseline and the stronger/stiffer Material2 fabric. By comparing Figs. 10–13 it is clear that, as the initial velocity of the projectile increases above 60 m/s, depending on friction conditions, there will be failure at the boundary prior to the failure of the yarns around the projectile for the stiffer/stronger Material2 – this effect is not manifest in the Kevlar KM2® baseline fabric. This initial boundary failure occurs about half-way through the process and is the first discontinuity in the projectile velocity vs. time graph shown in Fig. 12. Though yarns fail, there are still sufficient yarns connected to the boundary that – with friction – the fabric maintains enough integrity to continue slowing down the projectile. Clearly, for the stronger/stiffer Material2, boundary conditions are now coupling with the friction and material properties.

3.2. Effect of yarn material properties

In order to better understand the interaction between material properties, two other sets of material properties designated by Material3 and Material4 (see Table 2) were studied. Projectile velocity time histories reported in Fig. 14 correspond to the Kevlar KM2®, Material2, Material3 and Material4 fabrics under impact at $V_s = 80$ m/s. At this striking velocity, the Kevlar KM2® baseline fabric is expected to be penetrated whereas the Material2 fabric should defeat the projectile. For the simulations reported in Fig. 14, friction was introduced between the yarns as well as between the projectile and the fabric.

One can see that Material3 (lower stiffness but higher strength) was penetrated whereas Material4 (higher stiffness but lower strength) was not penetrated. As shown in Fig. 14, the projectile velocity profile for the Material3 fabric follows that of the Kevlar KM2® baseline until around 120 μ s after impact, since $E_{11}^{\text{Material3}} = E_{11}^{\text{Kevlar}}$. However due to the higher strength of Material3 yarns ($\sigma_1^{\text{Material3}} = 1.5\sigma_1^{\text{Kevlar}}$), the failure initiation time is somewhat delayed as the high-strength yarns are able to deform more and absorb a greater amount of the projectile's kinetic energy before

Table 3

Initial projectile velocity required to achieve near zero residual velocity under different friction parameters.

Friction	Range of initial velocity (m/s)	Interpolated initial velocity (m/s)
(a) Baseline Kevlar KM2® fabric: $E_{11} = 62$ GPa, $\sigma_1 = 3.4$ GPa		
Yarn–yarn and projectile–fabric	60–65	61
Only yarn–yarn	55–60	60
Only projectile–fabric	55–60	57
No friction	55–60	56
(b) Fabric woven with Material2 yarns: $E_{11} = 134$ GPa, $\sigma_1 = 4.9$ GPa		
Yarn–yarn and projectile–fabric	90–100	98
Only yarn–yarn	60–70	68
Only projectile–fabric	60–70	65
No friction	50–60	60

(a) The range and interpolated initial projectile velocity for the baseline Kevlar KM2® fabric. (b) The range and interpolated initial projectile velocity for the fabric assumed to be woven with Material2 yarns.

failure. Post-failure the projectile velocity profile for Material3 exhibits a second discontinuity around 185 μ s after impact that corresponds to yarn failure at the fixed boundaries. Effectively however, the post-failure projectile velocity profiles for both the Kevlar KM2® baseline and Material3 fabrics are parallel indicative of a net positive residual velocity corresponding to complete perforation. Therefore any further deceleration of the projectile beyond 200 μ s after impact, by either the Kevlar KM2® baseline or the Material3 fabric is due to the interaction of the projectile with the central yarn being pulled out (see Fig. 15a and c). The energy dissipation associated with the above event is appreciably lesser

in comparison with the case wherein the entire fabric is responsible for absorbing the projectile's kinetic energy. Therefore the magnitude of projectile deceleration beyond 200 μ s is significantly lesser in case of the above fabrics, as shown in Fig. 14. The snapshots in Fig. 15 indicate that the projectiles have perforated the corresponding targets, and in the case of Material3 (see Fig. 15c) also reveal yarn failure at the fixed boundaries.

Since $E_{11}^{\text{Material4}} = E_{11}^{\text{Material2}}$, the projectile velocity profile for the Material4 fabric follows that of the Material2 fabric until failure. However in this case failure occurs early and initiates at the boundaries. In fact, as seen in Fig. 15d, yarn failure near the impact

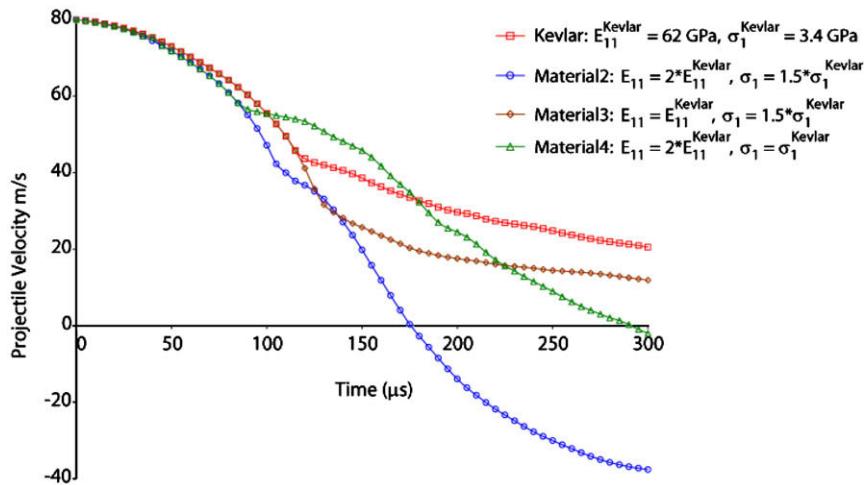


Fig. 14. The projectile velocity time history for impact events simulated on all the fabrics studied in this work.

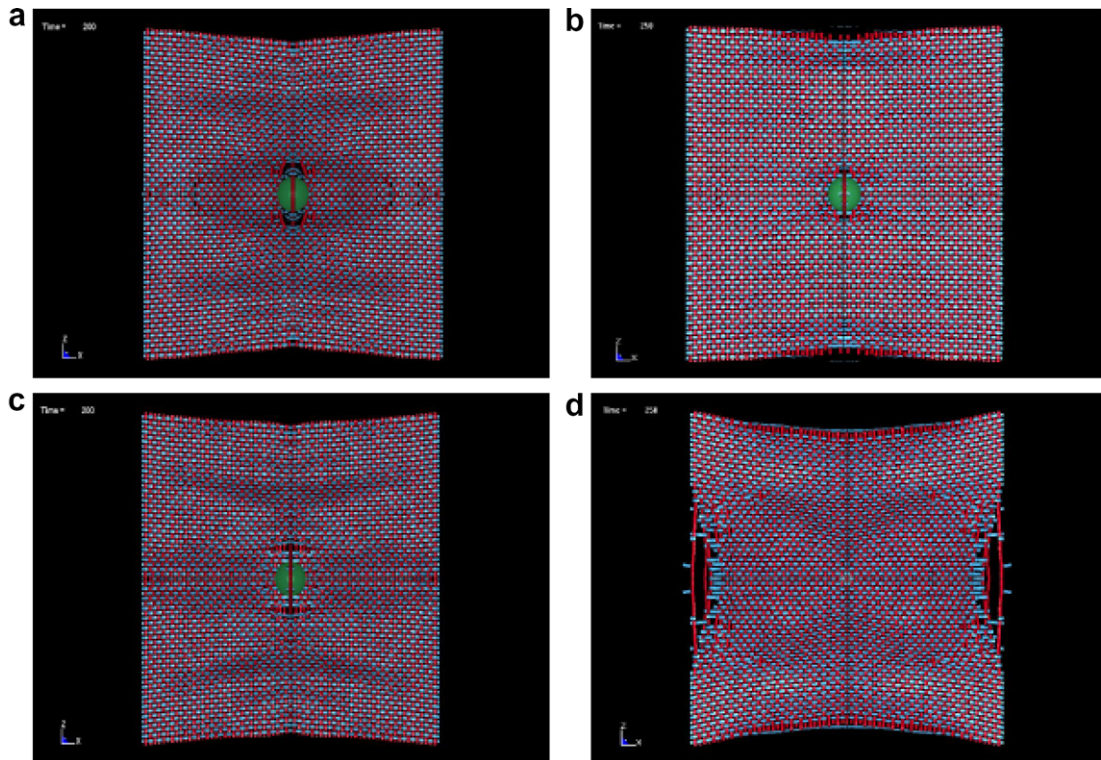


Fig. 15. The accumulated damage on the back face of fabrics studied in this work. The projectile impacts the fabrics at $V_s = 80 \text{ m/s}$. (a) Baseline Kevlar KM2® fabric at 200 μ s after impact. (b) Fabric woven with Material2 yarns at 250 μ s after impact. (c) Fabric woven with Material3 yarns at 200 μ s after impact. (d) Fabric woven with Material4 yarns at 250 μ s after impact.

region is almost undetectable in the Material4 fabric. By the end of simulation time (300 μ s), severe boundary failure of yarns is predicted as shown in Fig. 15d. Notwithstanding yarn failure at the fixed boundaries, with the aid of friction, the Material4 fabric is able to maintain its integrity leading to continuous slowing down of the projectile as shown in Fig. 14. Post-failure discontinuities in the projectile velocity profile are a result of successive yarn failures at the fixed boundaries.

Based on the results reported in Figs. 14 and 15, under projectile–fabric and yarn–yarn friction, and the two edges fixed – two edges free boundary conditions imposed, the simulations reported in this study imply that woven fabrics comprised of high stiffness and strength yarns provide better ballistic performance. As in the case of Material2 (see Fig. 14), the high stiffness lends to faster slowing down of the projectile, while the high-strength of the yarns allow them to deform more before failure thereby absorbing more of the projectile's kinetic energy. Friction in this case, helps to counter the boundary failure event by aiding the fabric to maintain its integrity by ensuring that sufficient yarns are connected at the boundary. Parametric studies on the effects of friction and boundary conditions were reported elsewhere [21].

4. Discussion

The above result is consistent with the literature. Cunniff [22] developed a qualitative comparative tool based on dimensional analysis, and Cunniff et al. [23] used the same with the objective of relating the ballistic performance of different armor systems. Based on that work [22], as one increases the stiffness and strength of the yarns (such as Material2 in this study), one could expect a relatively higher benefit toward improving ballistic performance than by merely increasing the strength of the yarns – as in the case of Material4 in this study. These results are supported by the projectile velocity time histories in Fig. 14 and increases in V_s as reported in Table 3. As shown in Fig. 14, at $V_s = 80$ m/s, the projectile penetrates the fabrics comprised of the baseline Kevlar KM2® and Material3 yarns, whereas it is stopped by fabrics comprised of Material2 and Material4 yarns. Reviewing the results in Table 3, it is clear that fabrics with Material2 yarns could actually stop a projectile at $V_s = 98$ m/s, implying that the benefit from increasing stiffness and strength outweighs the benefit from increasing strength of the yarns alone.

The exception to high fiber modulus and strength improving ballistic performance is embodied in comparing Kevlar® and carbon fibers. While carbon fibers are stiffer and stronger than Kevlar® fibers, their ballistic performance is much less desirable. Carbon fibers are characterized by a shear failure whereas Kevlar® fibers fail in tension [24], under ballistic impact. Therefore good ballistic materials as implied by the work of Cunniff [22] would be characterized by a tensile failure. Indeed, tensile failure further indicates the ability of the fiber/yarn to deform and absorb the kinetic energy of the projectile. A quantitative measure of the yarn's ability to absorb energy is the elastic strain energy which increases as the modulus is increased [25]. Therefore the results reported in this study are consistent with the mechanics of the problem.

5. Conclusions

As one would expect, for a given fabric geometry and projectile, material properties, boundary conditions and friction are coupled and all play a critical role in determining ballistic performance. The results reported in this study showed that friction aided in improving the ballistic performance of the fabric with higher stiffness and higher strength yarns, as indicated in Table 3. In addition, for that material, friction between yarns is clearly more important

than friction between projectile and the fabric, as also evident from the results in Table 3. Previous studies [8] showed that at striking velocities well above the ballistic limit of the fabric, projectile–fabric friction is more beneficial than yarn–yarn friction. These current results therefore, should be more applicable for fabrics operating near their ballistic limit.

Projectile velocity time histories in Figs. 12 and 14 indicate that fabrics comprised of high stiffness yarns (Material2 and Material4) decelerate the projectile faster, while fabrics comprised of high-strength yarns (Material3) result in the most delayed failure initiation time. However as shown in Fig. 12, the combination of high stiffness and strength (Material2), results in the most favorable ballistic performance under the imposed boundary conditions and frictional interactions. Additionally, fabrics comprised of Material2, Material3 and Material4 yarns are characterized by failure near the boundaries, as shown in Figs. 13 and 15. As such, one could consider designing boundary 'tiles' into the fabric comprised of high stiffness and strength yarns. This could provide additional energy-absorbing yarns at a 'boundary' while increasing sacrificial yarn breakage and at the same time maintaining the overall integrity of the fabric.

Clearly all of the parameters in a projectile–fabric ballistic event are inter-related and contribute to the performance of a fabric under impact. Models such as the one developed herein are critical to study ballistic impact as it is necessary to capture yarn–yarn interactions as well as projectile–fabric interactions. These types of models are necessary to better understand the couplings between the parameters which should lead to better flexible structures for ballistic protection.

Acknowledgements

The authors gratefully acknowledge the support of the United States Army Research Laboratory, Aberdeen Proving Ground, and the Center for Composite Materials, University of Delaware, during this research.

References

- [1] Tan VBC, Lim CT, Cheong CH. Perforation of high-strength fabric by projectiles of different geometry. *Int J Impact Eng* 2003;28(2):207–22.
- [2] Briscoe BJ, Motamedi F. The ballistic impact characteristics of aramid fabrics: the influence of interface friction. *Wear* 1992;158(1–2):229–47.
- [3] Bazhenov S. Dissipation of energy by bulletproof aramid fabric. *J Mater Sci* 1997;32(15):4167–73.
- [4] Zeng XS, Tan VBC, Shim VPW. Modelling inter-yarn friction in woven fabric armour. *Int J Impact Eng* 2006;66:1309–30.
- [5] Tan VBC, Ching TW. Computational simulation of fabric armour subjected to ballistic impacts. *Int J Impact Eng* 2006;32:1737–51.
- [6] Barauskas Rimantas, Abraitiene Ausra. Computational analysis of impact of a bullet against the multilayer fabrics in LS-DYNA. *Int J Impact Eng* 2007;34:1286–305.
- [7] Naik NK, Shrirao P. Composite structures under ballistic impact. *Compos Struct* 2004;66:579–90.
- [8] Tabiei Ala, Ivanov Ivelin. Computational micro-mechanical model of flexible woven fabric for finite element impact simulation. *Int J Numer Methods Eng* 2002;53:1259–76.
- [9] Duan Y, Keefe M, Bogetti T, Cheeseman B. Modeling friction effects on the ballistic impact behavior of a single-ply high-strength fabric. *Int J Impact Eng* 2005;31(8):996–1012.
- [10] Duan Y, Keefe M, Bogetti T, Cheeseman B, Powers B. A numerical investigation of the influence of friction on energy absorption by a high-strength fabric subjected to ballistic impact. *Int J Impact Eng* 2006;32(8):1299–312.
- [11] Duan Y, Keefe M, Wetzel ED, Bogetti TA, Powers B, Kirkwood JE, Kirkwood KM. Effects of friction on the ballistic performance of a high-strength fabric structure. In: International Conference on Impact Loading of Lightweight Structure 2005, May 8–12, Florianopolis, Brazil; 2005.
- [12] Yang HH. Aramid fibers compressive composite materials fiber reinforcements and general theory of composites. vol. 1. Oxford, UK.: Elsevier Science; 2000. 199–299.
- [13] Cheng M, Chen W, Weerasooriya T. Mechanical properties of Kevlar® KM2 single fiber. *J Eng Mater Technol* 2005;127(April):197–203.
- [14] Gu BH. Analytical modeling for the ballistic perforation of planar plain-woven fabric target by projectile. *Compos Part B-Eng* 2003;34(4):361–71.

- [15] Billon HH, Robinson DJ. Models for the ballistic impact of fabric armour. *Int J Impact Eng* 2001;25(4):411–22.
- [16] Parga-Landa B, Hernandez-Olivares F. An analytical model to predict impact behaviour of soft armours. *Int J Impact Eng* 1995;16(3):455–66.
- [17] Hallquist JO. LS-DYNA® theory manual. Livermore Software Technology Corporation 2006.
- [18] Cunniff PM. An analysis of the system effects in woven fabrics under ballistic impact. *Textile Res J* 1992;62(9):495–509.
- [19] Shim VPW, Tan VBC, Tay TE. Modeling deformation and damage characteristics of woven fabric under small projectile impact. *Int J Impact Eng* 1995;16(4):585–605.
- [20] Lim CT, Tan VBC, Cheong CH. Perforation of high-strength double-ply fabric system by varying shaped projectiles. *Int J Impact Eng* 2002;27(6):577–91.
- [21] Duan Y, Keefe M, Bogetti TA, Cheeseman BA. Modeling the role of friction during ballistic impact of a high-strength plain-weave fabric. *Compos Struct* 2005;68:331–7.
- [22] Cunniff Philip M. Dimensionless parameters for optimization of textile-based body armor systems. In: Proceeding of the 18th International Symposium on Ballistics, San Antonio, TX; 1999.
- [23] Cunniff Philip M, Auerbach Margaret A, Vetter Eugene, Sikkema Doetze J. High Performance M5 fiber for ballistics/structural composites. In: 23rd Army Science Conference, 2004.
- [24] Deitzel J. Private communication. Center for Composite Materials, University of Delaware.
- [25] Duan Y, Keefe M, Bogetti TA, Powers BM. Finite element modeling of transverse impact on a ballistic fabric. *Int J Mech Sci* 2006;48:33–43.